Theory of the single woodwind tone hole

Douglas H. Keefe[a)]
Department of Physics, Case Western Reserve University, Cleveland, Ohio 44106

(Received 27 March 1981; accepted for publication 15 April 1982)

A single tone hole may be generally represented in the transmission-line description of a woodwind musical instrument by a T-section circuit. This circuit element is comprised of a shunt and series impedance whose values differ depending on whether the hole is open or closed. The imaginary parts of these impedances have here been calculated as functions of frequency in terms of the main bore diameter, and the tone-hole chimney height and diameter. The loss-free wave equation is solved for a single tone hole placed through the wall of a cylindrical main bore. Green function expansions are made in both the main air column and tone hole. These two expansions must be equal on the surface of intersection between the main bore and tone hole, and this condition may be expressed by an integral equation over the surface. An approximate solution to the integral equation is obtained by Schwinger's variational formulation, and the impedance parameters in the T section are thereby computed and displayed in a form for use by musical acousticians. The series impedance for both open and closed holes is a negative inertance. The shunt impedance of a closed hole is a compliance which is simply related to the closed-hole volume. The shunt impedance of an open hole is written in terms of the open-hole effective length and expressed as a function of the tone-hole proportions.

PACS numbers: 43.75.Ef, 43.20.Mv, 43.20.Bi

INTRODUCTION

Woodwind musical instruments have a collection of tone holes at various positions on the main bore. The air column can be effectively shortened or lengthened by opening or closing these tone holes. The behavior of the woodwind is strongly affected by the tone-hole proportions,[1] and it is therefore of interest to understand the acoustic properties of a single tone hole joined onto the cylindrical main bore. This report presents theoretical formulas for the acoustic impedances which represent the presence of open- or closed-tone holes on a woodwind instrument. The assumptions underlying the validity of the formulation are that the excitation is described by the linearized equations of acoustics, and that the impedance parameters associated with each hole are independent of those of other holes. Paper II[2] discusses measurements of these tone-hole impedance parameters and the role of dissipation near the hole. Mutual impedance effects between tone holes and the presence of nonlinear acoustical streaming near tone holes are described elsewhere.[3]

The tone hole is a cylindrical tube of diameter $2b$ and height t which is joined onto the cylindrical main bore of diameter $2a$ as shown in Fig. 1. The z axis of the coordinate system runs along the midline of the main air column and $z=0$ is located at the center of the tone hole. The chimney height t of the tone hole is defined as the mean of the smallest and largest tone-hole heights t_1 and t_2, respectively. The tone-hole tube is perpendicular to the main bore on most woodwinds, and this is assumed to be the case in this report.

A convenient mathematical description of wave propagation within the main bore uses transmission-line theory. Since the tone-hole size is much less than a wavelength λ in the frequency range of interest, then the acoustic effect of the tone hole may be represented by means of a lumped circuit in the transmission-line equations. The most general form of this circuit may be represented as a T circuit with series and shunt impedance elements Z_a and Z_s, respectively (see Fig. 2). This use of the T circuit for both open- and closed-tone holes is slightly more general than has been employed in previous discussions concerning woodwind musical instrument.[4,5] The series and shunt impedances comprising the T circuit are calculated here by means of an approximate solution to the wave equation in the vicinity of the tone hole.

The series impedance acts in conjunction with the longitudinal particle velocity standing wave along the axis of the main air column at the tone-hole location, while the shunt impedance is related to the pressure standing wave directly under the hole. If the longitudinal flow (along the z direction in Fig. 1) is zero at the tone-hole location, then the pressure standing wave is symmetrical about the tone-hole center. For this symmetrical pressure distribution, only the shunt impedance Z_s in the lumped circuit plays a role, and the subscript s denotes this symmetry.

If there is a pressure node directly under the hole, then the series impedance Z_a of the T circuit is important. The

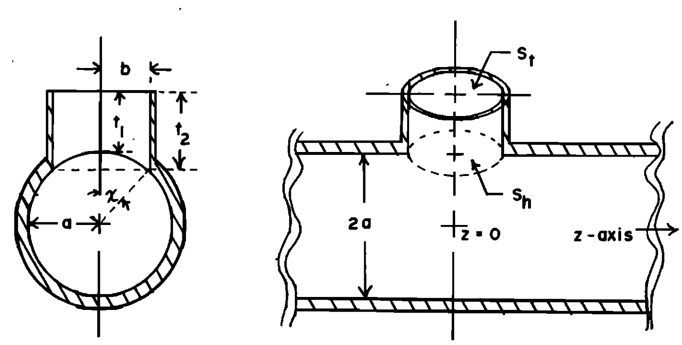

FIG. 1. Basic tone-hole geometry.

[a)] Present address: Cambridge Collaborative, Inc., P. O. Box 74, 169 Bent Street, Cambridge, MA 02142.

 0001-4966/82/090676-12$00.80

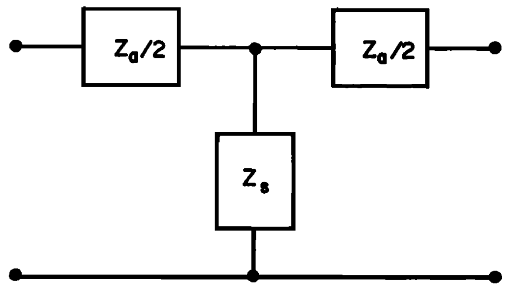

$$Z_s = R_0(a/b)^2 \begin{cases} -j\cot kt & \text{(CLOSED HOLE)} \\ jkt_e & \text{(OPEN HOLE)} \end{cases}$$

$$Z_a = R_0(a/b)^2(-j\,kt_a) \quad \text{(SAME FORM; OPEN, CLOSED)}$$

FIG. 2. T circuit element representing the tone hole in the transmission line.

TABLE I. Tone-hole impedance parameters.

Symbols	
a	Main bore radius
b	Tone-hole radius
t	Tone-hole chimney height
ρ	Density of air
c	Speed of sound (free space)
$R_0 = \rho c/\pi a^2$	Characteristic impedance of main bore
ξ_e	Total open-hole shunt resistance (see Paper II)[2]

Open-hole shunt impedance $Z_s^{(o)}$

$$Z_s^{(o)} = R_0(a/b)^2(jkt_e + \xi_e)$$

$$t_e(k) = \frac{(1/k)\tan kt + b\,[1.40 - 0.58\,(b/a)^2]}{1 - 0.61\,kb\tan kt} \text{ (see Paper II)}^2$$

$$\simeq (1/k)\tan kt + b\,[1.40 - 0.58(b/a)^2]$$

(no pad above hole)

closed-hole shunt impedance $Z_s^{(c)}$

$$Z_s^{(c)} = -jR_0(a/b)^2\cot kt$$

open-hole series impedance $Z_a^{(o)}$,

$$Z_a^{(o)} = R_0(a/b)^2(-jkt_a^{(o)})$$

$$t_a^{(o)} = \frac{0.47b\,(b/a)^4}{[\tanh(1.84t/b) + 0.62(b/a)^2 + 0.64(b/a)]}$$

closed-hole series impedance $Z_a^{(c)}$

$$Z_a^{(c)} = R_0(a/b)^2[-jkt_a^{(c)}]$$

$$t_a^{(c)} = \frac{0.47b\,(b/a)^4}{[\coth(1.84t/b) + 0.62(b/a)^2 + 0.64(b/a)]}$$

connection of the antisymmetry of the pressure standing wave with the series impedance is denoted by the subscript a. Since the average pressure over the tone-hole surface is zero for this case, then there is no *net* flow into or out of the hole.

The superscripts (c) and (o) indicate whether the tone-hole parameter of interest corresponds to a closed or open hole. For example, $Z_a^{(c)}$ is the series impedance in the lumped T circuit for a closed hole.

Before the detailed theory is discussed, the acoustic properties of tone holes and their relationship with the impedances in the lumped T-circuit representation are outlined. The shunt impedance for a closed-tone hole in the low-frequency limit is an acoustic compliance whose volume equals the closed-hole volume.[4] The series impedance for a closed-tone hole may be written as a negative length correction; that is, the presence of a closed-tone hole at a pressure node is equivalent to a reduction in the main bore length in the vicinity of the tone hole.[5] The theory outlined in this investigation shows that the series impedance for an open hole also has the form of a negative length correction, and the predicted value has a similar order of magnitude as the predicted closed-hole series impedance. The shunt impedance of an open hole in the absence of dissipation and with negligible radiation is an inertance which involves both inner and outer length corrections as well as the tone-hole chimney height.

Table I gives the imaginary parts of these four impedances. The open- and closed-hole series inertances and the open-hole shunt inertance are written in terms of length parameters $t_a^{(o)}, t_a^{(c)}$, and t_e, respectively. The open-hole length parameters include the flow-related effects at the inner junction of the tone hole with the main bore and the effect of the chimney height t on the inertances. Radiation from a tone hole is discussed in Paper II,[2] and the real parts of the impedances involving radiative, viscous, and thermal dissipation are also considered there. The present investigation concentrates on the mathematical physics underlying the derivation of the expressions in Table I.

Schwinger[6] introduced a powerful variational method within the context of electromagnetic waveguide theory to obtain an approximate solution to the loss-free wave equation. The variational method as used in this report is accurate as long as dissipation or nonlinear dynamics do not significantly alter the sound field except in the laminar boundary layer region.

An arbitrary disturbance within a waveguide may be expressed in terms of the normal modes of the waveguide. These include the plane-wave mode and the transverse-varying modes. At sufficiently low frequencies—in the range of major interest for woodwind acoustics—there is only a single normal mode which can transport energy over long distances within the duct. This single mode will often be called the fundamental mode of the duct, and it is the only normal mode for which any transverse cross section of the duct is an equipressure surface. All of the other modes will be referred to as secondary modes. In a smooth section of the duct, these secondary modes are the evanescent normal modes and the fundamental plane-wave mode is the propagating mode.

The acoustical disturbance at the discontinuity is separated into two parts (see Fig. 1)—an even part wherein the fundamental mode has even symmetry about the center of the tone hole and an odd part wherein the mode is antisymmetrical about the hole position $z = 0$. If the separate even and odd problems can be solved, then the total effect of the discontinuity can be represented as in Fig. 2. The representation of the lumped circuit element for this tone-hole discontinuity as an ABCD matrix[7,8] is given below, in the limit $|Z_a/Z_s| \ll 1$:

$$\begin{pmatrix} 1 & Z_a \\ 1/Z_s & 1 \end{pmatrix}. \tag{1}$$

The series impedance Z_a is determined from analysis of the antisymmetrical problem, and the shunt impedance Z_s from the symmetrical. It will be seen later and in experiments described in Paper II that the approximation $|Z_a/Z_s| \ll 1$ for woodwind tone-hole circuit T elements is well justified.

I. THEORETICAL FORMULATION

Let (r,ϕ,z) be the standard cylindrical coordinates along the main cylindrical air column and let $\psi(\mathbf{r})$ denote the velocity potential of the acoustical wave; that is,

$$v_z = \frac{\partial \psi}{\partial z}, \tag{2a}$$

$$p = -j\rho c k \psi. \tag{2b}$$

The wavenumber k equals ω/c, where the angular frequency ω is 2π times the oscillatory frequency f, and c is the speed of sound in free space. The coordinate r is the radial coordinate in any circular cross section of the main air column, and ϕ is the azimuthal coordinate. A Green function approach will be used to solve the boundary value problem (at least approximately), and the following fundamental theorem[9] is the basic starting point for setting up the boundary value problem for ψ in terms of the Green function G:

$$\psi(\mathbf{r}) = \int_V \rho(\mathbf{r}_0) G(\mathbf{r}|\mathbf{r}_0) dV + \int_{S_0} \{G(\mathbf{r}|\mathbf{r}_0)\nabla_0\psi(\mathbf{r}_0) - \psi(\mathbf{r}_0)\nabla_0 G(\mathbf{r}|\mathbf{r}_0)\}\cdot d\mathbf{S}_0, \tag{3a}$$

where ψ and G satisfy the inhomogeneous Helmholtz equation,

$$\nabla^2\psi + k^2\psi = -\rho \tag{3b}$$

$$\nabla^2 G(\mathbf{r}|\mathbf{r}_0) + k^2 G(\mathbf{r}|\mathbf{r}_0) = -\delta(\mathbf{r}-\mathbf{r}_0). \tag{3c}$$

V is the volume enclosing the observation point $\mathbf{r}_0$, S is the boundary of V, S_0 is the boundary enclosing the source, and

$$G(\mathbf{r}|\mathbf{r}_0) = G(\mathbf{r}_0|\mathbf{r}). \tag{4}$$

The volume integral over a source distribution ρ has given rise to the propagating mode $\psi_f(z)$, which depends only on the distance z along the duct. We always assume that the frequency of the excitation is sufficiently low so that there is only a single propagating mode in the smooth air column which we call the fundamental mode. It is convenient to choose Neumann boundary conditions for our Green function; that is

$$\frac{\partial G}{\partial n} = 0, \quad \text{on } S. \tag{5}$$

Under these conditions Eq. (4a) can be written as an integral equation over the surface S_h (see Fig. 1) which is the surface separating the main air column from the tone hole as follows:

$$\psi(\mathbf{r}) = \psi_f(z) + \int_{S_h} G(\mathbf{r}|\mathbf{r}_0)\left(\frac{\partial \psi(\mathbf{r}_0)}{\partial n_0}\right) dS_0 \tag{6}$$

(for $\mathbf{r}$ inside the main air column).

The above equation states that the total velocity potential $\psi(\mathbf{r})$ is the sum of the fundamental mode potential $\psi_f(z)$ plus an additional contribution which takes into account the flow into the open- or closed-tone hole. The term $\partial\psi/\partial n_0$ is the normal particle velocity through the inner surface of the tone hole. If the hole should "disappear" then $\partial\psi/\partial n_0 \rightarrow 0$, and $\psi(\mathbf{r})$ is equal to the fundamental mode potential $\psi_f(z)$.

The velocity potential $\psi(\mathbf{r})$ for points inside the tone hole is,

$$\psi(\mathbf{r}) = -\int_{S_h} G_h(\mathbf{r}|\mathbf{r}_0)\left(\frac{\partial \psi}{\partial n_0}\right)_{S_h} dS_0 + \int_{S_t} G_h(\mathbf{r}|\mathbf{r}_0)\left(\frac{\partial \psi}{\partial n_0}\right)_{S_t} dS_0 \tag{7}$$

(for $\mathbf{r}$ inside the tone hole). In the above relation, G_h is the Green function for propagation inside the cylindrical tone hole of radius b; $(-\partial\psi/\partial n_0)|_{S_h}$ is the particle velocity *into* the tone hole (which accounts for the minus sign); S_t is the circular surface at the outside termination of the tone hole (see Fig. 1) and $(\partial\psi/\partial n_0)|_{S_t}$ is the velocity *out* of the tone hole. The normal derivative of the velocity potential $(\partial\psi/\partial n_0)|_{S_t}$ is zero at the termination of a *closed* hole (if the porosity and compliance of the pad which closes the hole on a woodwind instrument are ignored) so that Eq. (7) simplifies to

$$\psi(\mathbf{r}) = -\int_{S_h} G_h(\mathbf{r}|\mathbf{r}_0)\left(\frac{\partial \psi}{\partial n_0}\right)\Bigg|_{S_h} dS_0 \tag{8}$$

(for $\mathbf{r}$ inside the closed-tone hole). If the tone hole is open, the normal velocity at the outside edge of the hole involves the radiation impedance, and discussion on that additional complication is deferred until Sec. IVB.

Equation (6) gives the velocity potential for points inside the main air column, and Eq. (8) gives it for points inside the closed-tone hole. This pair of equations is known as a dual integral equation, and a variational formulation[10] is chosen to compute an approximate solution. Hart and Cantrell[11] consider a problem where the fundamental mode is antisymmetrical about the tone-hole center, and their approach suggested the variational treatment used here. Schwinger and Saxon[12] discuss the reduction of the general problem into even and odd cases.

Until further notice, the tone hole is assumed to be *closed* by a rigid termination. For points on the surface S_h which bounds both the main air column and the tone hole (see Fig. 1), the expressions for the velocity potential $\psi(\mathbf{r})$ in Eqs. (6) and (8) must be equal; therefore we have

$$-\int_{S_h} G(\mathbf{r}|\mathbf{r}_0)\left(\frac{\partial \psi}{\partial n_0}\right) dS_0 = \psi_f(z) + \int_{S_h} G(\mathbf{r}|\mathbf{r}_0)\left(\frac{\partial \psi}{\partial n_0}\right) dS_0, \tag{9a}$$

or

$$0 = \psi_f(z) + \int_{S_h} \{G(\mathbf{r}|\mathbf{r}_0) + G_h(\mathbf{r}|\mathbf{r}_0)\}\left(\frac{\partial \psi}{\partial n_0}\right) dS_0 \tag{9b}$$

(for r on S_h).

Equation (9b) is a key integral equation in the variational method, and is valid only for points $\mathbf{r}$ on the surface of intersection S_h between the air column and the closed-tone hole.

A. Odd symmetry: Variational expression and series impedance representation of discontinuity as a circuit element

Suppose that the velocity potential or the pressure of the propagating mode is antisymmetrical about the hole position $z=0$. Then we may write the velocity potential $\psi_f(z)$ of the fundamental mode in terms of the amplitude P of the pressure as follows:

$$\psi_f(z) = (j/\rho ck)P \sin kz. \tag{10}$$

We evaluate the velocity potential in Eq. (6) at a length $z=l$, where l is sufficiently large that all the secondary modes excited at the discontinuity are negligible. In practice, it is sufficient that l be larger than the diameter $2a$ of the main air column. At a distance $z \gg l$, we can approximate the Green function G in Eq. (6) by that part $G^{(f)}$ of the Green function which depends only on the fundamental mode plane-wave excitation. This is shown in Sec. II A [see Eq. (42)] to be

$$G^{(f)}(z|z_0) = (1/\pi a^2 k)e^{-jkz} \sin kz_0 \tag{11}$$

(for $z \gg z_0 \gg 0$). Hence for z larger than z_0, Eq. (6) for the velocity potential simplifies to

$$\psi(z) = (j/\rho ck)P \sin kz + (c/\pi a^2 k)e^{-jkz} \times \int_{S_h} F(z_0,\phi_0) \sin kz_0 \, dS_0. \tag{12}$$

The normal particle velocity $\partial\psi/\partial_0$ on the surface S_h has been written for convenience in terms of a dimensionless function $F(z_0,\phi_0)$ as follows:

$$\frac{\partial\psi}{\partial n_0} \equiv cF(z_0,\phi_0). \tag{13}$$

The admittance Y_l is defined to be the ratio of outgoing volume flow u_l to the pressure p_l at $z=l$, and is written below in terms of the velocity potential:

$$Y_l \equiv \frac{u_l}{p_l} = j\left(\frac{\pi a^2}{\rho c}\right)\left(\frac{1}{k}\right)\left(\frac{\partial\psi}{\partial z}\Big/\psi\right)_{z=l}. \tag{14}$$

The above equation and Eq. (12) imply that

$$Y_l R_0 = \frac{j \cos kl - j(\rho c^2/P)K_a e^{-jkl}}{\sin kl - j(\rho c^2/P)K_a e^{-jkl}}, \tag{15a}$$

where

$$R_0 \equiv (\rho c/\pi a^2), \tag{15b}$$

is the wave impedance of the cylindrical main air column of radius a, and where the dimensionless quantity K_a (the subscript denoting the present case of antisymmetry) is defined to be

$$K_a \equiv \left(\frac{1}{\pi a^2}\right) \int_{S_h} F(z_0,\phi_0) \sin kz_0 \, dS_0. \tag{16}$$

The quantity K_a contains all the information on the presence of the discontinuity as long as one is observing in a region where the evanescent mode contributions are negligible. As a point of clarification, Eq. (15a) does not imply that the admittance Y_l depends upon the pressure amplitude P or the length l. The term K_a scales with the magnitude of $F(z_0,\phi_0)$, or, equivalently, the magnitude of the particle velocity into the tone hole. This velocity is in turn scaled by the pressure amplitude P, so that the quantity $(\rho c^2/P)K_a$ is independent of the overall pressure amplitude.

The next step is to express the series impedance Z_a, defined in Sec. I A, in terms of the admittance Y_l looking down the main air column at $z=l$. By assumption, the fundamental pressure mode has a node at $z=0$ corresponding to the pressure being antisymmetrical about the tone hole. Thus, looking backwards from $z=l$ to $z=0$, the pressure and flow at the two places are related by the product of the ABCD matrix over a distance $(-l)$ terminated by the series impedance at the origin as follows:

$$\begin{pmatrix} p_l \\ -u_l \end{pmatrix} = \begin{pmatrix} \cos kl & -jR_0 \sin kl \\ (-j/R_0)\sin kl & \cos kl \end{pmatrix} \times \begin{pmatrix} 1 & Z_a \\ 0 & 1 \end{pmatrix} \begin{pmatrix} 0 \\ u(z=0) \end{pmatrix}. \tag{17}$$

This formula is valid for arbitrary l and is evaluated, for the sake of convenience, for kl equal to an odd number of quarter wavelengths. This is allowable since the tone-hole series impedance is independent of l. Manipulation of Eq. (17) leads to the following relation between Z_a and Y_l:

$$p_l/(-u_l) = R_0^2/Z_a,$$

or

$$Y_l R_0 = -Z_a/R_0. \tag{18}$$

Under these conditions, Eqs. (15a) and (18) lead to an expression for the series impedance in terms of the discontinuity function K_a:

$$\frac{Z_a}{R_0} = \frac{(\rho c^2/P)K_a}{1-(\rho c^2/P)K_a}. \tag{19}$$

As was mentioned earlier, the effect of a discontinuity placed at the pressure node of an acoustical wave in a duct is described using the series impedance Z_a, and this, in turn, depends on an accurate calculation of K_a to which attention is now turned.

B. Calculation of K_a via the variational approach

We cannot compute K_a without knowing the velocity $cF(z_0,\phi_0)$ into the hole. The flow function F is chosen by means of a variational calculation which leaves K invariant under small changes in F.

Begin by multiplying Eq. (9b) by $cF(z,\phi)$ and integrating over S_h to obtain:

$$0 = j\left(\frac{P}{\rho c^2}\right)\left(\frac{1}{k}\right) \int_{S_h} F(z,\phi) \sin kz \, dS + \int_{S_h} dS \int_{S_h} dS_o \, F(z,\phi)\{G(\mathbf{r}|\mathbf{r}_0) + G_h(\mathbf{r}|\mathbf{r}_0)\}F(z_0,\phi_0). \tag{20}$$

This equation and Eq. (16) imply that

$$0 = \pi a^2 K_a - jk\left(\frac{\rho c^2}{P}\right) \int_{S_h} dS \, F(z,\phi) \times \int_{S_h} dS_0 \, F(z_0,\phi_0)\{G + G_h\}. \tag{21}$$

The trick in obtaining the variational formulation depends on adding Eqs. (21) and πa^2 times Eq. (16). This step leads to an expression in which one factor of K_a is placed on the left-hand side of the equation as follows:

$$\pi a^2 K_a = 2\int_{S_h} F(z_0,\phi_0)\sin kz_0\, dS_0 - jk\left(\frac{\rho c^2}{P}\right)\int_{S_h} dS\, F(z,\phi)$$
$$\times\int_{S_h} dS_0\, F(z_0,\phi_0)\{G+G_h\}. \tag{22}$$

Suppose that some physically reasonable trial function is chosen for F, and suppose it differs from the "exact" function F_0—whatever that might be. The error in choosing F naturally leads to an error in K_a in the above equation. We demand that the first-order variation δK_a in the discontinuity function be zero for a first-order variation δF in F; that is,

$$0 = \pi a^2 \delta K_a = 2\int_{S_h} dS\, \delta F\left[\sin kz - jk\left(\frac{\rho c^2}{P}\right)\right.$$
$$\left.\times\int_{S_h} dS_0\, F(z_0,\phi_0)\{G+G_h\}\right]. \tag{23}$$

The symmetry of either Green function under the interchange of coordinates [see Eq. (4)] has been used in deriving the above expression. Moreover, the integrand which multiplies δF in the above is seen from Eqs. (9b), (10), and (13) to be identically zero. That is, K_a is stationary if F is exactly equal to its true value F_0.

Let the choice of trial flow function be a constant B times a function $f(z_0,\phi_0)$ whose magnitude is of order unity (actually, the magnitude of f is of no consequence as will be seen). Then the variation of F from its exact value F_0 is

$$\delta F = Bf - F_0. \tag{24}$$

We look for an approximate solution to Eq. (23) such that δK_a remains zero. This constraint leads to a value for the constant B.

Substitute the approximate value Bf of the flow function in Eq. (23), use Eq. (24) for δF, and make use of the fact that the exact function F_0 satisfies Eq. (23) identically. It follows that δK_a is zero if and only if

$$0 = \pi a^2 \delta K_a = 2B\left[\int_{S_h} dS\, f(z,\phi)\sin kz\right.$$
$$\left. - jkB\left(\frac{\rho c^2}{P}\right)\int_{S_h} dS\, F(z,\phi)\int_{S_h} dS_0 f(z_0,\phi_0)\{G+G_h\}\right]. \tag{25}$$

Solving the above for the constant B gives the result,

$$B = \frac{\displaystyle\int_{S_h} dS \sin kz\, f(z,\phi)}{\displaystyle\left(\frac{jk\rho c^2}{P}\right)\int_{S_h} dS\, f(z,\phi)\int_{S_h} dS\,\{G+G_h\} f(z_0,\phi_0)}. \tag{26}$$

Equations (26) and (16) give the desired expression for K_a to be,

$$\left(\frac{\rho c^2}{P}\right)K_a = \frac{\displaystyle\left(\frac{-j}{\pi a^2 k}\right)\left(\int_{S_h} dS \sin kz f(z,\phi)\right)^2}{\displaystyle\int_{S_h} dS\, f(z,\phi)\int_{S_h} dS_0\{G+G_h\} f(z_0,\phi_0)}. \tag{27}$$

The first thing about Eq. (27) to note is that the value of K_a is independent of the magnitude of the trial function f. More importantly, a first-order error in the choice of the feed-in function f leads to only a second-order error in the discontinuity function K_a since K_a is stationary with respect to f.

To summarize, a trial function f is chosen based upon prior knowledge of what the tone-hole geometry and acoustical wave excitation are like. The integrals in Eq. (27) are evaluated to obtain K_a, and the impedance Z_a is calculated from Eq. (19). As an important aside, since the acoustical disturbance at the discontinuity has the same symmetry as the fundamental mode, it follows that $f(z,\phi)$ must be antisymmetrical in z since $\psi_f(z)$ is. Applications of Eq. (27) to the closed- and open-hole impedance calculations are presented in Secs. III and V.

C. Even symmetry: Variational expression and shunt impedance

The argument in this section runs a parallel course to the discussion of the antisymmetrical case in the previous section. Therefore, only the highlights are touched upon. When the pressure or velocity potential is symmetrical about the tone hole, the velocity is at a node; hence the effect of the discontinuity can be entirely represented as a shunt admittance in the one-dimensional transmission-line equations. The tone hole is symmetrically placed about $z=0$, and the fundamental mode ψ_f of the velocity potential is written as

$$\psi_f(z) = (j/\rho ck)P\cos kz. \tag{28}$$

Equation (6) for the velocity potential becomes

$$\psi(\mathbf{r}) = \left(\frac{j}{\rho ck}\right)P\cos kz + c\int_{S_h} G(\mathbf{r}|\mathbf{r}_0)F(\mathbf{r}_0)dS_0. \tag{29}$$

The above equation is evaluated for points $z \gg l$, where l is larger than the length scale of evanescent mode disturbances, and the only contribution from the Green function is that of the fundamental mode. Moreover, the fundamental mode Green function $G^{(f)}(z|z_0)$ must be symmetrical about z_0 since the acoustic wave is symmetrical, and the correct Green function turns out to be [see Eq. (41) of Sec. II A],

$$G^{(f)}(z|z_0) = (-j/\pi a^2 k)e^{-jkz}\cos kz_0. \tag{30}$$

$(z \geqslant z_0 \geqslant 0)$.

Equations (29) and (30) show that the velocity potential far from the tone hole is

$$\psi(z) = \left(\frac{j}{\rho ck}\right)P\cos kz - \left(\frac{jc}{\pi a^2 k}\right)e^{-jkz}\int_{S_h} dS_0 \cos kz_0 F(\mathbf{r}_0). \tag{31}$$

The acoustic admittance Y_l at a distance $z=l$ along the main air column is derived from Eqs. (14) and (31) with the result,

$$Y_l R_0 = j\left(\frac{-\sin kl + je^{-jkl}(\rho c^2/P)K_s}{\cos kl - (\rho c^2/P)e^{-jkl}K_s}\right), \tag{32}$$

where the discontinuity function K_s associated with this symmetrical case is defined to be

$$K_s \equiv \left(\frac{1}{\pi a^2}\right)\int_{S_h} F(z_0,\phi_0)\cos kz_0\, dS_0. \tag{33}$$

When the admittance in Eq. (32) is evaluated at kl equal to an integral number of half-wavelengths, the transmission line at $z = l$ appears to be terminated at $z = 0$ by a shunt impedance Z_s equal to

$$\frac{Z_s}{R_0} = \frac{1 - (\rho c^2/P)K_s}{(\rho c^2/P)K_s}. \tag{34}$$

A parallel argument to the discussion in Sec. I C leads to a variational expression for K_s which is accurate to second order as long as the trial function f, defined in Eq. (24) is accurate to first order; and the result for K_s is

$$\left(\frac{\rho c^2}{P}\right)K_s = \frac{\left(\frac{-j}{\pi a^2 k}\right)\left(\int_{S_h} dS \cos kz\, f(z,\phi)\right)^2}{\int_{S_h} dS\, f(z,\phi) \int_{S_h} dS_0 \{G_h + G_e\} f(z_0,\phi_0)}. \tag{35}$$

This equation is identical to the expression Eq. (27) for K_a (the antisymmetric case discontinuity function) except for the substitution of the cosine for the sine function. Again, the integrals in Eq. (35) must be carried out before the shunt impedance Z_s can be evaluated.

II. CONSTRUCTION OF THE GREEN FUNCTIONS

A. The Green function for the main air column

In order to evaluate K_a and K_s in Eqs. (27) and (35) we need to construct a solution of Eq. (3c) under the condition that the normal velocity at the wall, $r = a$, is zero. Inspection of Eq. (6) shows that the Green function G must have the same even or odd symmetry in z that the fundamental mode pressure excitation has.

The Green function for a point excitation inside a smooth cylindrical duct of radius a is known to be,[13]

$$G(r,\phi,z|r_0,\phi_0,z_0) = \left(\frac{-j}{2\pi a^2}\right) \sum_{m=0}^{\infty} \epsilon_m \cos m(\phi - \phi_0) \times \sum_{n=0}^{\infty} \frac{J_m(\mu_{mn} r/a) J_m(\mu_{mn} r_0/a) e^{-j\kappa_{mn}|z - z_0|}}{\kappa_{mn} [J_m(\mu_{mn})]^2 [1 - (m/\mu_{mn})^2]}, \tag{36}$$

where

$$\epsilon_m \equiv \begin{cases} +1 & m = 0 \\ +2 & m > 0 \end{cases}. \tag{37}$$

The radial eigenvalues μ_{mn} are determined from the boundary condition that the radial derivative of the Green function, and hence of the mth-order Bessel function J_m, be zero at $r = a$.

TABLE II. Values of Bessel eigenvalues μ_{mn} for m, $n < 2$.

	$n =$	0	1	2
$m =$	0	...	3.83	7.02
	1	1.84	5.33	8.53
	2	3.05	6.71	9.97

Values of the first few μ_{mn} are listed in Table II. The (m,n) wavenumber κ_{mn} in the axial direction is equal to

$$\kappa_{mn} \simeq -j(\mu_{mn}/a)[1 - (ka/\mu_{mn})^2]^{1/2}, \quad \simeq -j(\mu_{mn}/a), \quad \text{for } ka \ll 1 \tag{38}$$

except when $m = n = 0$, for which case it is equal to

$$\kappa_{00} = k. \tag{39}$$

At low frequencies, which include the musically relevant frequencies, κ_{mn} is pure imaginary for all air column modes other than the fundamental $m = n = 0$ mode. The (m,n) evanescent mode amplitude is attenuated by $1/e$ in a distance λ_{mn} equal at low frequencies to

$$\lambda_{mn} = (a/\mu_{mn}). \tag{40}$$

Thus all evanescent modes are negligible over a length comparable to one or two duct diameters.

The dependence of G upon z_0 is contained in the factor,

$$g(z|z_0) = e^{-j\kappa|z - z_0|}$$

with the appropriate κ. It has been mentioned that the Green function must have the correct even or odd symmetry in z, and this requirement is satisfied by the use of image source theory.[14] A suitable linear combination of sources of unit amplitude at z_0 and $-z_0$ gives the Green functions $g_s(z|z_0)$, for the symmetric case, and $g_a(z|z_0)$ for the antisymmetric case as follows:

$$g_s(z|z_0) = e^{-j\kappa|z - z_0|} + e^{-j\kappa|z + z_0|},$$
$$g_a(z|z_0) = e^{-j\kappa|z - z_0|} - e^{-j\kappa|z + z_0|}.$$

Restricting attention to the region where $z + z_0 > 0$, the above equations can be written as

$$g_s(z|z_0) = \begin{cases} e^{-j\kappa z} 2 \cos \kappa z_0, & z > z_0 \\ e^{-j\kappa z_0} 2 \cos \kappa z, & z < z_0 \end{cases}$$

$$g_a(z|z_0) = \begin{cases} e^{-j\kappa z} 2j \sin \kappa z_0, & z > z_0 \\ e^{-j\kappa z_0} 2j \sin \kappa z, & z > z_0. \end{cases}$$

We obtain the result that the Green function G_s (or G_a) inside the main cylindrical air column when the velocity potential is symmetrical (or antisymmetrical) about the tone hole centered at $z = 0$, is

$$G_s(r,\phi,z|r_0,\phi_0,z_0) = \left(\frac{-j}{\pi a^2 k}\right) e^{-jkz} \cos kz_0 + \left(\frac{1}{\pi a}\right) \sum_{m,n=0}^{\infty\,\prime} \frac{\epsilon_m \cos(\phi - \phi_0) J_m(\mu_{mn} r/a)}{\mu_{mn} [J_m(\mu_{mn})]^2 [1 - (m/\mu_{mn})^2]} \times J_m\left(\frac{\mu_{mn} r_0}{a}\right) e^{\mu_{mn} z/a} \cosh\left(\frac{\mu_{mn} z_0}{a}\right), \quad (\text{for } z > z_0), \tag{41}$$

$$G_a(r,\phi,z|r_0,\phi_0,z_0) = \left(\frac{1}{\pi a^2 k}\right) e^{-jkz} \sin kz_0 + \left(\frac{1}{\pi a}\right) \sum_{n,m=0}^{\infty\,\prime} \frac{\epsilon_m \cos m(\phi - \phi_0) J_m(\mu_{mn} r/a)}{\mu_{mn} [J_m(\mu_{mn})]^2 [1 - (m/\mu_{mn})^2]} \times J_m\left(\frac{\mu_{mn} r_0}{a}\right) e^{-\mu_{mn} z/a} \sinh\left(\frac{\mu_{mn} z_0}{a}\right), \quad (\text{for } z > z_0). \tag{42}$$

We have separated out the fundamental mode portion of the Green function from the evanescent secondary mode contributions, and these fundamental mode Green functions appeared in Eqs. (11) and (30). The prime on the summation sign in Eqs. (41) and (42) signifies that the sum is over all m and n except $m=n=0$.

It is appropriate to conclude this section with a discussion of how to represent the inner surface of the tone hole—the surface of integration S_h referred to earlier (see Fig. 1)—in terms of the coordinates (r,ϕ,z). Two views of the air column and tone hole are shown in Fig. 1. The tone hole has a circular cross section of inner diameter $2b$, and the geometric length t is chosen to be the mean of the smallest distance t_1 and the largest distance t_2 from the top of the tone hole to the point where the tone hole joins the main bore. The parameter t is defined in this way, since it turns out that it is very efficient to measure t_1 and t_2 on an actual instrument and take the mean value; t_1 is the "carpenter's thickness" of the air column cylinder.

The inner surface of integration S_h and the terminating surface of integration S_t are both shown in Fig. 1. The latter surface S_t is a circle of radius b. The surface S_h is, unfortunately, more complicated, being a saddle-shaped surface defined by the coordinates

$$\begin{aligned}&r=a, \quad -b\leqslant z\leqslant b,\\ &-\arcsin[(b^2-z^2)/a^2]^{1/2}\leqslant\phi\leqslant\arcsin[(b^2-z^2/a^2]^{1/2}.\end{aligned} \tag{43}$$

In the above, the line $z=\phi=0$ passes through the tone-hole center, and the maximum value of ϕ, denoted by χ in Fig. 1 equals arc $\sin(b/a)$. Since the tone-hole radius b is smaller than the main bore radius a, then it is permissible to use the small angle approximation and write the limits of integration of the coordinate ϕ as

$$-[(b^2-z^2)/a^2]^{1/2}\leqslant\phi\leqslant[(b^2-z^2)/a^2]^{1/2}. \tag{44}$$

In this approximation, the surface S_h has an area of πb^2, the same as S_t. All of the integrals in the relations for the discontinuity function which are evaluated in this coordinate system use the small angle approximation for the integration limits of ϕ.

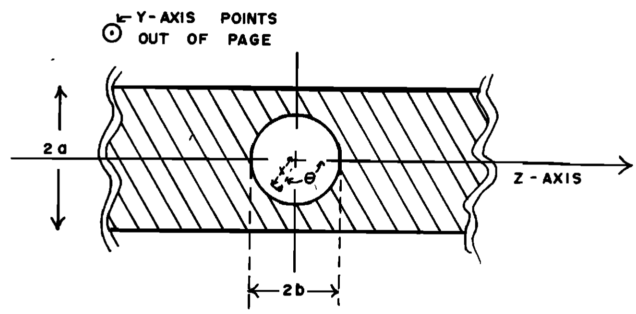

FIG. 3. Tone-hole coordinates. A top view is shown looking down on the main air column through the tone hole.

B. The Green function for the tone hole

The coordinates for points inside the tone hole are chosen such that x is the radial coordinate, θ is the angular coordinate, and y is the coordinate for propagation along the main axis of the duct (see Fig. 3). The coordinate θ which varies from 0 to 2π is measured from the $+z$ axis of the main duct; that is, the line along $\theta=0$ and perpendicular to the tone-hole axis is the $+z$ axis of the main bore. The tone hole begins at $y=0$, which corresponds to $r=a-\frac{1}{2}(t_2-t_1)$ in the main bore.

For any of the integrals evaluated over the surface S_h in this coordinate system, the small angle approximation in which S_h is taken to be a flat surface is used. Hence the surface S_h in this coordinate system is represented as

$$y=0, \quad 0\leqslant\theta\leqslant 2\pi, \quad 0\leqslant x\leqslant b. \tag{45}$$

The Green function for propagation within the tone hole can be immediately adapted from Eq. (37) with the substitution of the coordinates (x,θ,y) for (r,ϕ,z), respectively. The Green function G_h for a point source is

$$\begin{aligned}G_h(x,\theta,y|x_0,\theta_0,y_0)=&\left(\frac{-j}{2\pi b^2k}\right)e^{-jk|y-y_0|}+\left(\frac{1}{2\pi b}\right)\sum_{n,m=0}^{\infty\,\prime}\frac{\epsilon_m\cos m(\theta-\theta_0)J_m(\mu_{mn}x/b)}{\mu_{mn}[J_m(\mu_{mn})]^2[1-(m/\mu_{mn})^2]}\\ &\times J_m\left(\frac{\mu_{mn}x_0}{b}\right)e^{-(\mu_{mn}/b)|y-y_0|}, \quad (\text{for } kb\ll\mu_{10}).\end{aligned} \tag{46}$$

The boundary condition that $\partial G/\partial x$ be zero at the tone-hole wall $(x=b)$ is satisfied by choosing μ_{mn} to have the same value as has been defined already. However, the normal derivative $\partial G/\partial y_0$ at either end of the tone hole must also vanish, namely

$$\left(\frac{\partial G_h}{\partial y_0}\right)_{y_0=0}=0, \quad \left(\frac{\partial G_h}{\partial y_0}\right)_{y_0=t}=0.$$

We again introduce image sources in order to meet these boundary conditions, but since there are a pair of conditions rather than a single condition to be satisfied, the image problem is more complicated. There turn out to be an infinite number of images (see Morse and Feshbach[15] for a related discussion), but they can be summed for our limited purposes. We take the source point y_0 at some arbitrary point inside the tone hole. To obtain a zero gradient $(\partial/\partial y)$ of G_h at $y=0$, an image is placed at $-y_0$; to obtain a zero gradient at $y=t$, an image is placed at $2t-y_0$. This first pair of images is labeled in Fig. 4 along with the original source at y_0. However, we need to place two more images in order to counterbalance the first pair, and so on.

An important simplification occurs when it is noticed that in Eqs. (27) and (35) for the discontinuity functions K_a and K_s, the tone-hole Green function G_h is evaluated only at

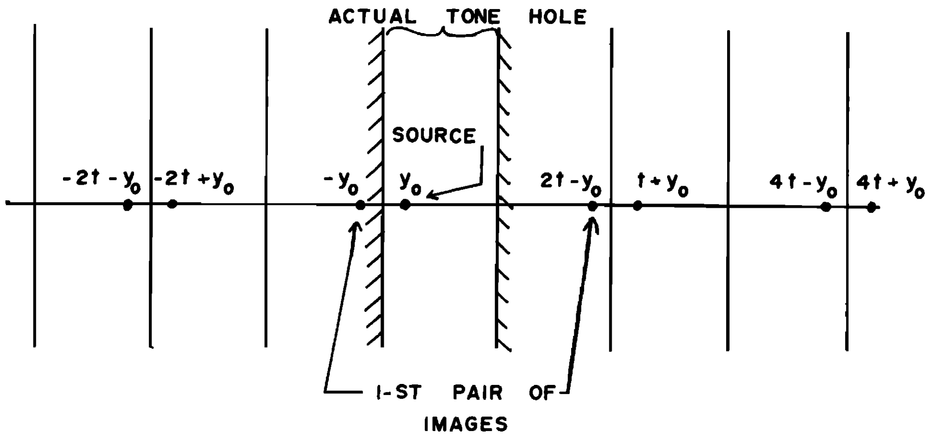

FIG. 4. Open tone-hole image sources. The tone hole of height t is shown between the hatched lines, and the source at y_0 and its first few images are illustrated.

points on S_h where $y = y_0 = 0$. It is easy to see from Fig. 4, that as y_0 approaches zero, a double image forms at $y_0 = 0, \pm 2t, \pm 4t, \ldots$. Thus the factor $e^{-j\kappa|y-y_0|}$ in Eq. (46) is replaced by a term $h'(y|0)$ is given by

$$e^{-j\kappa|y-y_0|} \rightarrow h'(y|0) = 2 \sum_{l=-\infty}^{\infty} e^{-j\kappa|y-2lt|}. \tag{47a}$$

Moreover, when we set $y = 0$ in the above as is the case for G_h on the surface S_h, the series can be split up into a sum over positive and negative values of l. Each sum is a geometric series, and the final replacement term $h'(y|0)$ is

$$\begin{aligned} h'(y|0) &= -2j \cot \kappa t \\ &= +2 \coth(\mu t/b), \quad \text{for } \kappa = -j\mu/b. \end{aligned} \tag{47b}$$

Therefore, the Green function G_h, to be used in the variational calculation, is

$$\begin{aligned} G_h|_{S_h} &\equiv G_h(x,\theta,y=0|x_0,\theta_0,y_0=0) = \left(\frac{-1}{\pi b^2 k}\right)\cot kt + \left(\frac{1}{\pi b}\right) \\ &\times \sum_{n,m=0}^{\infty\,\prime} \frac{\epsilon_m \cos m(\theta-\theta_0) J_m(\mu_{mn}x/b)}{\mu_{mn}[J_m(\mu_{mn})]^2[1-(m/\mu_{mn})^2]} \\ &\times J_m(\mu_{mn}x_0/b) \coth(\mu_{mn}t/b). \end{aligned} \tag{47c}$$

III. CLOSED-HOLE SERIES IMPEDANCE

The three integrals to be evaluated in order to compute the closed hole antisymmetric discontinuity function $K_a^{(c)}$ in Eq. (27); the superscript (c) or (o) is used to denote the closed or open hole, respectively. The impedances are

$$I_1 = \int_{S_h} dS\, f(z,\phi) \sin kz, \tag{48a}$$

$$I_2 = \int_{S_h} dS \int_{S_h} dS_0\, G_a(r=a,\phi,z|r_0=a,\phi_0,z_0)\, f(z_0,\phi_0), \tag{48b}$$

$$I_3 = \int_{S_h} dS \int_{S_h} dS_0\, G_h(x,\theta,y=0|x_0,\theta_0,y_0=0) f(x_0,\theta_0). \tag{48c}$$

In the above, substitution is made for G_a from Eq. (42) and G_h from Eq. (47c). The discontinuity function $K_a^{(c)}$ is given in terms of these integrals by

$$K_a^{(c)} = \left(\frac{P}{\rho c^2}\right)\left(\frac{-j}{\pi a^2 k}\right)\frac{[I_1]^2}{[I_2+I_3]}. \tag{49}$$

The following realistic feed-in function is chosen:

$$f(z,\phi) = z, \tag{50a}$$

or, equivalently,

$$f(x,\theta) = x \cos \theta. \tag{50b}$$

This function is the simplest possible function both continuous and antisymmetrical about $z = 0$, as is required. The three integrals have been computed[3] for this choice of feed-in function and the results are,

$$I_1 = \pi/4(kb)b^3, \tag{51a}$$

$$I_2 = 0.421b^5 \coth(1.84t/b), \tag{51b}$$

$$I_3 = 0.259b^5(b/a)^2[1-0.733]jkb + 0.679b^5\mathscr{E}, \tag{51c}$$

where

$$\mathscr{E} \simeq 0.4(b/a). \tag{52}$$

The discontinuity function is computed from Eq. (49) and the above integrals, and the tone-hole series impedance $Z_a^{(c)}$ for the closed hole is found from Eq. (19) to be

$$Z_a^{(c)} = R_0(a/b)^2(-jkt_a^{(c)}). \tag{53}$$

The length parameter $t_a^{(c)}$ is,

$$\begin{aligned} t_a^{(c)} = b\,&[0.47(b/a)^4][\coth(1.84t/b) \\ &+ [0.62(b/a)^2 + 0.64(b/a)]. \end{aligned} \tag{54}$$

That there is a series impedance for a closed-tone hole which has the form of a negative inertance was pointed out by Nederveen and van Wulfften Palthe.[5] Physically, the spreading of the flow so as to penetrate slightly into the tone-hole cavity decreases the kinetic energy density, and this effect is represented in the transmission line by the negative inertance. It will be shown later that the *open* hole located at a pressure node is also represented by a series negative inertance in the transmission-line equations. These impedance parameters and their application to musical woodwinds are discussed in Paper II.

As a final note, the calculations of the closed-hole series impedance were also carried out for the following alternate choice of feed-in function:

$$f(z,\phi) = \begin{cases} +1, & z>0 \\ -1, & z<0 \end{cases}. \tag{55}$$

Comparison with Eq. (50) shows that both functions have the appropriate antisymmetry, although the function f in Eq. (50) has the advantage of being continuous at $z=0$. The results obtained using Eq. (55) have the same functional dependence as those in Eq. (54). The numerial coefficients differ only slightly—on the order of 20% at most.

IV. OPEN-HOLE SHUNT IMPEDANCE

A. Preliminaries

The next case considered is the open-hole shunt impedance, which is the open-hole impedance when the fundamental mode of the main air column is symmetrical about the tone-hole position. This case is perhaps the most important from a practical standpoint, since the tone holes radiate most strongly into the room when the pressure is a maximum directly underneath. In the low-frequency limit ($kb \ll 1$) the impedance is written as

$$Z_s^{(o)} = jR_0(a/b)^2 Ekb, \tag{56}$$

where the real positive quantity E multiplied by b is the open-hole length correction.

There are two limiting expressions for E. When $t \gg b$, the secondary evanescent-type modes excited at the inside surface S_h of the tone hole have been strongly attenuated by the time they have reached the outside terminating surface S_t of the tone hole, and similarly for the nonpropagating modes excited at S_t (see Fig. 1). It is therefore possible to consider separate inner and outer length correction factors E_i and E_o, respectively, since the two ends of the tone hole are not coupled. In the other limiting form, $t \ll b$, it is not *a priori* evident whether it is proper to consider the end correction factor E to be separately composed of an inner and outer factor; nevertheless, an exact solution in the limit of zero frequency and negligible t exists which will be later used to refine the variational calculation of the open-hole shunt inertance.

The limit of t small compared to the radius b is appropriate for woodwind instruments which have large diameter and short chimney holes (e.g., saxophone or Boehm flute tone holes); and the limit of t comparable to or larger than $2b$ refers to small diameter and tall chimney holes (e.g., clarinet). This convention applies equally well to cylindrical or conical bore instruments, since the bore diameter of conical bore woodwinds does not vary much over the length of a tone-hole diameter.

Consider the clarinet-type case for which the chimney height is on the order of the tone-hole diameter. The outer length correction, discussed in Paper II,[2] is taken to be the radiation impedance associated with the radiation from an unflanged tube.[16] This correction factor is

$$E_o = 0.6133. \tag{57}$$

The inner length correction factor E_i is calculated below in terms of the tone-hole proportions.

For the large diameter, short chimney sax-type holes, we use the additional inertance associated with a constriction of negligible thickness ($t \to 0$) whose radius b is much less than a wavelength. Morse and Ingard[17] give the low-frequency limit of the length correction factor to be

$$E = \pi/4 + 0.6133 = 1.40, \quad (\text{for } t \ll b). \tag{58}$$

The first term on the right-hand side of the above is the exact expression at zero frequency to account for the diverging flow around the tone hole. This term is important in the later discussion of the variational calculation. The second term is the radiative correction factor E_o.

B. Variational formulation for the open-tone hole

In the earlier discussion of the variational methods, the velocity potential inside the tone hole was given by a surface integral over the inner tone-hole surface S_h and the outer surface S_t [see Eq. (7)]. The surface integral over S_t was zero when the hole was closed since the normal flow is zero at the termination. However, this integral is nonzero when the hole is open. Equation (7) illustrates that the Green function $G_h(\mathbf{r}|\mathbf{r}_0)$ for propagation inside the tone hole is evaluated on the surface S_t; i.e., for points where $y_0 = t$.

The form of the Green function derived in Eq. (46) was for a point source located at y_0, and the dependence of G_h upon y and y_0 was represented in the factor $h(y|y_0)$ as follows:

$$h(y|y_0) = e^{-jk|y-y_0|}. \tag{59a}$$

The twin requirements that $\partial G_h/\partial y_0$ be zero at $y_0=0$ and $y_0=t$ led to the introduction of an infinite number of images as shown in Fig. 4. We needed to evaluate G_h at $y_0=0$ in order to compute the integral over S_h, whereas in the present case we also need to evaluate G_h on the surface S_t where $y_0=t$. It is easy to see from Fig. 4 that, in the limit that y_0 approaches t, images of double strength form at $y_0 = \pm t, \pm 3t, \pm 5t, \ldots$, so that h is replaced by h', where h' is given by

$$h \to h'(y|y_0) = 2\sum_{l=-\infty}^{\infty} e^{-jk|y-(2l+1)t|}. \tag{59b}$$

Equation (7) also shows that we must evaluate the flow through S_t which occurs in the integral over S_t. Let u_h and u_t denote the volume flow through S_h and S_t, respectively. To the extent that the magnitude of the radiation impedance is small ($|Z_r/R_0| \ll 1$), these flows are related by the following ABCD matrix:

$$\begin{pmatrix} p_h \\ u_h \end{pmatrix} = \begin{pmatrix} \cos kt & jR_0(a/b)^2 \sin kt \\ (j/R_0)(b/a)^2 \sin kt & \cos kt \end{pmatrix} \begin{pmatrix} u_t Z_r \simeq 0 \\ u_t \end{pmatrix}$$

so that

$$u_t = u_h/\cos kt.$$

It follows that the particle velocities on S_h and S_t are approximately related by,

$$\left(\frac{\partial\psi}{\partial n_0}\right)_{S_t} = \left(\frac{\partial\psi}{\partial n_0}\right)_{S_h} \Big/ \cos kt. \tag{60a}$$

We may therefore rewrite Eq. (7) as

$$\begin{aligned} \psi(x,\theta,y) = -\int \{ & G_h(x,\theta,y|x_0,\theta_0,y_0=0) \\ & - [G_h(x,\theta,y|x_0,\theta_0,y_0=t)/\cos kt]\} \\ & \times \left(\frac{\partial\psi}{\partial n_0}\right)_{S_h} dS_0. \end{aligned} \tag{60b}$$

The net effect of the additional surface integral over the outside surface of the tone hole is to replace G_h evaluated at

$y_0 = 0$ by a difference in the tone-hole Green functions evaluated at the entrance and exit of the tone hole, $y_0 = 0$ and t, respectively.

In the variational expressions for the symmetric and antisymmetric discontinuity functions K_s and K_a, G_h must be evaluated at the observation point $y = 0$. Thus we set y equal to zero in Eq. (59b), and carry out the sum to obtain

$$h'(y=0|y_0=t) = 2\sum_{l=1}^{\infty} e^{-jk(2l-1)t} + \sum_{l=0}^{\infty} e^{-jk(2l+1)t}, \\ = -2j/\sin kt. \tag{60c}$$

Equations (60c) and (47a,b) show that the difference in Green functions which occurs in Eq. (60b) evaluated at $y = 0$ involves the term

$$\begin{aligned} h'(y=0|y_0=0) &- \frac{h(y=0|y_0=t)}{\cos kt} \\ &= -2j\cot kt + \left(\frac{2j}{\sin kt}\right)\left(\frac{1}{\cos kt}\right), \\ &= \begin{cases} 2j\tan kt \\ 2\tan k(\mu t/b), & \text{if } k = -j(\mu/b). \end{cases} \end{aligned} \tag{60d}$$

Therefore, the appropriate Green function G_h in the open-hole case to be used in the calculation of the discontinuity functions given in Eqs. (27) and (35) is

$$\begin{aligned} G_h^{(o)}(x,\theta,|x_0,\theta_0) &= (1/\pi b^2 k)\tan kt\,(1/\pi b) \\ &\times \sum_{m,n=0}^{\infty\,\prime} \frac{\epsilon_m \cos m(\theta-\theta_0) J_m(\mu_{mn}x/b)}{\mu_{mn}[J_m(\mu_{mn})]^2[1-(m/\mu_{mn})^2]} \\ &\times J_m(\mu_{mn}x_0/b)\tanh(\mu_{mn}t/b). \end{aligned} \tag{60e}$$

This equation is the counterpart for an open hole to the Green function in Eq. (47c) for the closed-hole case. The logical steps leading up to the derivation of the analogous expressions to Eqs. (27) and (35) have not been repeated for this open-hole case, but it may readily be verified that the only change is the above substitution of the tone-hole Green function. Basically, the $-j$ cot or coth functions associated with the closed-hole case have been replaced by a $+j$ tan or tanh functions, respectively, for the open-hole case.

C. Calculation of the open-hole shunt impedance: even symmetry

When the pressure is a maximum underneath the tone hole, the flow through S_h will be symmetrical about the z axis. The most physically reasonable yet analytically amenable flow pattern through the hole to use is the flow through an aperture in the zero frequency limit—this is just the solution to Laplace's equation under the boundary condition that the flow normal to an infinite plane is zero except inside a circular region of radius b. This flow pattern is nearly constant over the center of the circle and it gets very large near the edge of the hole up to the viscous boundary layer. It is precisely this flow which leads to the low-frequency length correction factor given in Eq. (58).

The simplest possible feed-in function $f(x,\theta)$ for a symmetrical flow, is chosen namely that the flow through the inner hole surface is constant. As before, the coordinate x is the radial coordinate over the nearly circular surface S_h. The exact low-frequency flow field discussed in the above paragraph departs from a constant value in that it has a quadratic dependence on x.

The flow through the hole expressed in terms of the functions F and f, and the constant B defined in Eqs. (13) and (24) is

$$\frac{\partial\psi}{\partial n_o} = cF(x_0,\theta_0) = cBf(x_0,\theta_0), \tag{61a}$$

$$f(x_0,\theta_0) = \begin{cases} 1, & \text{r on } S_h \\ 0, & \text{otherwise} \end{cases}. \tag{61b}$$

Equation (35) gives the symmetric discontinuity function K_s and it simplifies for the case that the feed-in function f is taken to be unity to,

$$\left(\frac{\rho c^2}{P}\right)K_s = \left(\frac{-j}{\pi a^2 k}\right)\left[\left(\int_{S_h} dS\cos kz\right)^2 \Big/ \left(\int_{S_h} dS \int_{S_h} dS_0\{G_h^{(o)} + G_s\}\right)\right]. \tag{61c}$$

A test of the reasonableness of this feed-in function will be to compare the impedance calculated via the variational expression for K_s, to the exact limiting form (t and kb small) implied by Eqs. (56) and (58) to be,

$$Z_{\text{exact}} = jR_0(a/b)^2(\pi/4)kb, \quad \text{for } kb \ll 1 \text{ and } t \simeq 0. \tag{62}$$

The variational expression will show the additional effect of the tone-hole chimney height.

The three integrals in Eq. (16c) have been calculated[3] using Eqs. (41) and (60e) for G_s and $G_h^{(o)}$, respectively. The results to second order in frequency are

$$\int_{S_h} dS\cos kz = \pi b^2[1 - \tfrac{1}{8}(kb)^2], \tag{63a}$$

$$\int_{S_h} dS \int_{S_h} dS_0\, G_h^{(o)} = \left(\frac{\pi b^2}{k}\right)\tan kt, \tag{63b}$$

$$\int_{S_h} dS \int_{S_h} dS_0\, G_s = -j\pi\left(\frac{b}{a}\right)^2\left(\frac{b^2}{k}\right)[1 - \tfrac{1}{4}(kb)^2 \\ - 0.58jkb] + 3.61b^3. \tag{63c}$$

The tone-hole impedance associated with the change in flow due to the presence of the hole is evaluated from Eqs. (34), (35), (61c), and (63) and is found to be pure imaginary to order $(kb)^2$, so that

$$Z_s^{(o)} = jR_0(a/b)^2 kt_s^{(o)}, \tag{64a}$$

$$t_s^{(o)}(k) = \{(1/k)\tan kt + b[(3.61/\pi) - 0.58(b/a)^2]\}. \tag{64b}$$

The low-frequency limit of the tone-hole length correction parameter $t_s^{(o)}(k)$ for (b/a) very small is

$$t_s^{(o)}(0) = (3.61/\pi)b + t. \tag{65a}$$

If we take the chimney height to be negligible, then

$$t_s^{(o)}(0) \rightarrow (3.61/\pi)b. \tag{65b}$$

We have already argued that the exact form of $t_s^{(o)}$ in the limit that t and k go to zero is

$$t_{\text{exact}} = (\pi/4)b. \tag{65c}$$

The discrepancy between Eqs. (65b) and (65c) is due to the various approximations in carrying out the integrals and the infinite summations which therein occur. In line with this expectation, Eq. (64b) is replaced by an expression in which the low-frequency and zero t limit is explicitly satisfied as follows:

$$t_s^{(o)}(k) = (1/k)\tan kt + b\,[\pi/4 - 0.58(b/a)^2]. \tag{66}$$

The shunt impedance representation of this open-hole discontinuity is to lowest order the sum of the impedance calculated above with the radiation impedance. Higher-order frequency corrections are discussed in Paper II.[2] Equations (57) and (66) give the total length correction $t_s^{(o)}$, denoted by the effective length t_e, to be

$$t_e = (1/k)\tan kt + (\pi/4)b\,[1 - 0.74(b/a)^2] + 0.6133b. \tag{67a}$$

The second and third terms on the right-hand side of the above are the inner and outer length corrections, respectively. For frequencies such that $kt \ll 1$, the effective length t_e is

$$t_e = t + b\,[1.40 - 0.58(b/a)^2]. \tag{67b}$$

Of course, the actual physical situation is the main bore coupled to the tone hole, which is in turn to the geometry of the exterior of the instrument and the room enclosing it all. In addition, many open-tone holes have keys and pads suspended above the hole in the nearfield of the tone-hole source. Despite these complexities, experiments to be described in Paper II[2] show that the low-frequency formula for the open-hole effective length as given in Eq. (67b) closely approximates the actual acoustical behavior of a woodwind open-tone hole. The open-hole shunt impedance must be modified to include a resistive dissipative term.

V. OPEN-HOLE SERIES IMPEDANCE

The open-hole series impedance is obtained quite easily from the closed-hole series impedance expressions. The antisymmetry about $z = 0$ is introduced through the same choice of trial function f as in Eqs. (50) for the closed-tone hole. The only change in the open-hole calculation[3] in the integrals I_1, I_2, I_3 to be evaluated from Eq. (48), is that the open-tone-hole Green function $G_h^{(o)}$ derived in Eq. (60e) is used in Eq. (48c) for the integral I_3 instead of the closed-hole Green function. This substitution only very slightly changes the calculation of I_3 from that for the closed hole. The calculations of I_1 and I_2 are identical for both the closed and open holes.

The series open-tone-hole impedance $Z_a^{(o)}$ is evaluated using Eqs. (19) and (27), and the computations of the integrals in Eq. (48) subject to the modifications discussed above with the result:

$$Z_a^{(o)} = R_0(a/b)^2(-jkta^{(o)}), \tag{68a}$$

where

$$t_a^{(o)} = \frac{0.47b\,(b/a)^4}{[\tanh(1.84t/b) + 0.62(b/a)^2 + 0.64(b/a)]}. \tag{68b}$$

The series impedance for the open- and closed-tone holes, Eqs. (68) and (54), respectively, are identical except for the replacement of a coth by a tanh function.

In the limit that $(1.84\,t/b)$ becomes large—a tall chimney, small diameter hole—the series impedances Z_a for the open and closed holes approach the same value. This is to be expected since all the modes excited in the tone-hole chimney are evanescent. For t sufficiently large, the evanescent modes have become negligible at the outside of the hole and there is essentially no acoustic disturbance at the outside edge of the hole, be it open or closed. It is also apparent that the open tone-hole series impedance is always a negative inertance, as in the closed-hole case.

In the opposite short chimney limit such that $(1.84\,t/b)$ is small, then the open hole at the pressure *node* can still radiate, though as a *dipole* rather than a monopole acoustic source. This is because the acoustic motion on either side of the center model line of the hole are out of phase. This dipole radiation is non-negligible only for large diameter holes such as those on the saxophone.

VI. CLOSED-HOLE SHUNT IMPEDANCE

The closed-hole shunt impedance $Z_s^{(c)}$ is simply obtained from the open-tone-hole shunt impedance formulation. Eq. (61c) for the discontinuity function K_s is the same for the open and closed holes except that the Green function $G_h^{(c)}$ in Eq. (47c) for the closed hole is used instead of $G_h^{(o)}$. The calculations[3] are analogous to those described earlier and the results for the imaginary part of the closed-hole shunt impedance $Z_s^{(c)}$ are

$$\begin{aligned} Z_s^{(c)} &= -jR_0(a/b)^2\{\cot kt + kt\,[\tfrac{1}{3}(b/t)^2 \\ &\qquad + 0.58(b/a)^2 - (\pi/4)(b/t)\}], && (69a) \\ &= -jR_0(a/b)^2 \cot kt, \quad \text{for } kt \ll \cot kt, && (69b) \\ &= -j(\rho c^2/\omega V), \quad \text{for } kt \ll 1. && (69c) \end{aligned}$$

For tone holes on most musical woodwind instruments, only the cot kt term in the above is important, and the low-frequency limit is equivalent to the statement[4] that the bore has effectively been increased in volume by the amount $V = \pi b^2 t$ equal to the tone-hole volume. The very tall chimney holes found on the bassoon form an exceptional case. Equation (69a) predicts that an additional inner length correction factor is involved for these tall chimney holes at higher frequencies.

VII. SUMMARY

The series and shunt impedance elements in the lumped T circuit representing the acoustic effect of the tone hole in the transmission line have been evaluated in terms of the tone-hole proportions under the assumption that acoustic dissipation is negligible. This T circuit may be included in transmission-line models of woodwinds at the position of each tone hole on the main bore of the instrument.

ACKNOWLEDGMENTS

The research reported here is based upon a doctoral dissertation completed by the author at Case Western Reserve University. Arthur H. Benade, my advisor, helped greatly in all stages of my work from the initial formulation of the problem to a critical reading of this manuscript. I wish to thank the National Science Foundation for supporting this research.

[1]A. H. Benade, *Fundamentals of Musical Acoustics* (Oxford U. P., New York, 1976).
[2]D. H. Keefe, J. Acoust. Soc. Am. **72**, 676–687 (1982).
[3]D. H. Keefe, *Woodwind Tone Hole Acoustics and the Spectrum Transformation Function* (University Microfilms, Ann Arbor, 1981). Ph.D. dissertation, Case Western Reserve University, pp. 277–289. The calculation of the integrals is also available from the author as report R1.
[4]A. H. Benade, J. Acoust. Soc. Am. **32**, 1591–1608 (1960).
[5]C. Nederveen and D. W. van Wulfften Palthe, Acustica **13**, 65–70 (1963).
[6]J. Schwinger and D. Saxon, *Discontinuities in Waveguides* (Gordon and Breach, New York, 1968).
[7]J. J. Karakash, *Transmission Lines and Filter Networks* (Macmillan, New York, 1950).
[8]M. Lampton, Acustica **39**, 239–251 (1978).
[9]P. Morse and U. Ingard, *Theoretical Acoustics* (McGraw–Hill, New York, 1968), p. 321.
[10]Reference 9, p. 155, 679.
[11]R. W. Hart and R. H. Cantrell, J. Acoust. Soc. Am. **35**, 18–24 (1963).
[12]Reference 6, pp. 1–37.
[13]P. Morse and H. Feshbach, *Methods of Theoretical Physics*, 2 vols. (McGraw–Hill, New York, 1953), II, pp. 1563–65.
[14]Reference 9, pp. 366–369.
[15]Reference 13, I, pp. 812–815.
[16]H. Levine and J. Schwinger, Phys. Rev. **74**, 958–974 (1949).
[17]Reference 9, p. 481.
[18]U. Ingard, J. Acoust. Soc. Am. **25**, 1037–1061 (1953).